Automatic EEG Artifact Removal Techniques by Detecting Influential Independent Components

Sim Kuan Goh, Hussein A. Abbass, *Senior Member, IEEE*, Kay Chen Tan, *Fellow, IEEE*, Abdullah Al-Mamun, *Senior Member, IEEE*, Chuanchu Wang, *Member, IEEE*, and Cuntai Guan, *Senior Member, IEEE*

***Abstract*—Electroencephalography (EEG) data are used to design useful indicators that act as proxies for detecting humans' mental activities. However, these electrical signals are susceptible to different forms of interferences—known as artifacts—from voluntarily and involuntarily muscle movements that greatly obscure the information in the signal. It is pertinent to design effective artifact removal techniques (ARTs) capable of removing or reducing the impact of these artifacts. However, most ARTs have been focusing on handling a few specific types, or a single type, of EEG artifacts. EEG processing that generalizes to multiple types of artifacts remains a major challenge. In this paper, we investigate a variety of eight different and typical artifacts that occur in practice. We characterize the spatiotemporal-frequency influence of these EEG artifacts and offer two heuristics. The proposed heuristics extend influential independent component analysis to clean the contaminated EEG signal. These proposed heuristics are compared against four state-of-the-art EEG ARTs using both real and synthesized EEG, collected in the presence of multiple artifacts. The results show that both heuristics offer superior spatiotemporal-frequency performance in automatic artifacts removal and are able to reconstruct clean EEG signals.**

***Index Terms*—Brain computer interface, electroencephalography, EEG artifact removal techniques, independent component analysis, wavelet analysis.**

I. Introduction

RECENT advances in the area of Brain Computer Interfaces (BCIs) [1] have helped the disabled to improve their ability to communicate and control external devices through real–time psychophysiological measurements. Most BCIs make use of electroencephalography (EEG) to capture brain electrical activities using sensors/electrodes [2], [3]. The recorded EEG arises from synchronized neural activities, produced by the firing of neurons in the brain. Some applications require a mesh of electrodes, quantitative electroencephalograph (QEEG), to simultaneously acquire signals from multiple locations spread over the scalp. Decoding the QEEG signals [4] into high-order cognitive states, such as emotions [5], memory [6] and planning, is a key step towards the design of more advanced BCI systems. These systems need to be suitable for both medical applications and naturalistic settings, including safety critical decision making environments, such as real-time management of air traffic controllers' workload [7], [8].

Any conclusion drawn from EEG signals depends on how much organic brain signal activities are captured by the signal. The primary challenge in capturing true brain activities lies in the existence of non-brain source electrical activities, known as artifacts, that greatly distort EEG recording. Artifacts are induced by normal human voluntarily and involuntarily activities such as eye movements and muscle contractions.

The development of artifacts removal techniques can be broadly categorized into three classes known as 3R: reduce, reject and recover. Artifacts prevention [9], [10] is widely followed in EEG experiments to reduce the occurrence of artifacts, however, in principle, even under a very conditioned experimental environment, a human can't control against artifacts for a long time. The simplest and most intuitive approach to handle the undesired artifacts is by rejecting contaminated EEG segments from the recording [9], [10] to ensure that conclusions are drawn only from reliable data. Nevertheless, this comes at the expense of large information loss [11]. The ideal 'R' for EEG analysis is signal recovery to improve both the quality and quantity of EEG information. Existing techniques for recovering EEG signal from artifacts can be classified [12] based on the number of EEG channels being simultaneously used for artifacts removal. The first group includes regression, filtering, wavelet, and empirical mode decomposition (EMD). These methods work on a single channel. The second group is known as blind source separation (BSS) and work on multiple channels simultaneously.

Regression and filtering such as linear regression [13], [14], adaptive filtering [15]–[17], Wiener filtering [15] and Bayes filtering [15], [18], [19] use or estimate the reference channel of artifacts using additional channels. These methods have the advantage of working on a single channel automatically. However,

Manuscript received November 5, 2016; revised February 5, 2017 and March 1, 2017; accepted March 24, 2017. Date of current version August 7, 2017. *(Corresponding author: Sim Kuan Goh.)*

S. K. Goh and A. A. Mamun are with the Department of Electrical and Computer Engineering, National University of Singapore, Singapore 117583 (e-mail: simkuan@u.nus.edu; eleaam@nus.edu.sg).

H. A. Abbass is with the School of Engineering and Information Technology, University of New South Wales, Canberra, ACT 2600, Australia (e-mail: hussein.abbass@gmail.com).

K. C. Tan is with the Department of Computer Science, City University of Hong Kong, Hong Kong (e-mail: kaytan@cityu.edu.hk).

C. Wang is with the Institute for Infocomm Research, Agency for Science Technology and Research (A*STAR), Singapore 138632 (e-mail: ccwang@i2r.a-star.edu.sg).

C. Guan is with the School of Computer Science and Engineering, College of Engineering, Nanyang Technological University, Singapore 639798, and also with the Institute for Infocomm Research, Agency for Science Technology and Research (A*STAR), Singapore 138632 (e-mail: CTGuan@ntu.edu.sg).

Digital Object Identifier 10.1109/TETCI.2017.2690913

these techniques require a proper calibration before the experiment and either an extra reference or an estimated one to capture artifacts. The latter requirement can hardly be achieved in EEG data that are contaminated by multiple artifacts [12].

Wavelet [20] and EMD [21] model the time-frequency or temporal-oscillatory of a single channel. Since an artefact has different time-frequency characteristics compared to EEG, the wavelet basis or intrinsic mode of EEG artifacts can be removed from the signal [22]–[28].

BSS, also known as component analysis has the advantage of estimating artifacts' signals using a multivariate approach, with all EEG channels being used. The most common methods rely on, principle component analysis [29], canonical correlation analysis [30], and independent component analysis (ICA) [31]–[33]. ICA is considered the most reliable method when prior knowledge on artifacts is unknown [12]. The estimation of independent components and their qualities have gained significant attention in the literature [34]–[36]. For example, clustering and visualization are common techniques to investigate the reliability of independent components [37]. Different implementations of ICA have been proposed in the literature; one of the most common of which is Extended Infomax ICA [38], which has been investigated in many papers [39], [40]. EEG signals are passed through an ICA. Through visual inspection by a human, contaminated components are removed and the signal is reconstructed using the remaining components [41]. However, visual inspection is a time consuming task. With the vast amount of data collected today in QEEG settings, it is near to impossible to visually inspect these data. Automated methods to process the data reduce, or eliminate, human involvement.

Many other ARTs such as BSS with wavelet [23], [24] and BSS with EMD [42], [43] are designed based on some combinations of the above methods. There are also methods that hybridize with algorithms from statistics [44] and machine learning [40], [45], [46] to achieve automatic artifacts removal. While many work have been devoted to this artifact removal problem, the robustness of ARTs in the scenario of multiple artifacts remains to be a challenging problem because of the restrictive prior assumption made on an EEG artifact will fail to generalize to handle artifacts from different origins (eye, mouth, neck), subjects and electrode placements.

The contributions of this work are: (1) Characterizing the spatiotemporal-frequency influence of multiple EEG to study and synthesize artifacts. (2) Validating the reliability and robustness of existing methods for automatic artifacts removal by designing eight different EEG experiments and performing three EEG artifact simulations. (3) We also attempt to compare two of our proposed methods $H1$ and $H2$, that model and manipulate the influence of EEG artifact through influential independent components, against four state-of-the-art ARTs in Section II. The proposed methods were found to be more flexible to generalize to different type of artifacts and contributed a better EEG signal reconstruction.

The rest of this paper is organized as follows: Section II presents a brief overview of related work on EEG ARTs, with a focus on methodologies that work in conjunction with ICA where proposed methods will be compared to. This is followed by Section III, where two of our proposed ARTs are discussed. In Section IV, the validation scheme for evaluating ARTs is discussed, and the synthesis of EEG artifacts, EEG experiments along with results are presented in Sections V, VI and VII, respectively. Conclusions are drawn in Section VIII.

II. Related Work

Independent component analysis (ICA) has been widely used to de-mix signals collected from multiple sources. The de-mixing or separation process is based on a linear transformation of the mixed signals into maximally statistically independent components.

The ICA decomposition addresses the problems where data can be formulated as $X = AS + N$, where X denotes measured signals, A denotes mixing matrix, N denotes noise and S denotes Sources. Mathematically, ICA performs linear transformation W from mixed signals to components such that the components are statistically independent and with non-gaussian distribution, $\hat{S} = WX + N$. Once W and the estimated sources $\hat{S}$ are found, A can be obtained from the inverse of W. Being an independent event of neural signals, artifact sources can be separated into components. The cleaner EEG signals can be reconstructed from those components deemed useful: $\hat{X} = W^{-1}\hat{S}$. Visual inspection by clinical experts can always be carried out to detect and remove those independent components being suspected to be contaminated with artifacts. A number of ICA algorithms have been successfully used for EEG analysis [47] and ARTs [48]. These include SOBI [34], Infomax ICA [35] and FastICA [36]. ICA has also been used as the basis for a number of heuristics and methodologies designed for EEG artifacts removal. Among these, probably the most commonly used methods in the literature are FASTER [44], ADJUST [40], MARA [45], and wICA [23].

FASTER [44] is an unsupervised methodology that detects artifacts by analyzing various statistical properties of the data: channels, epochs, independent components, single-channel single-epochs, and aggregated data. It assumes that the statistical measurements underlying what defines a correct signal are normally distributed. It then detects and rejects signals' outliers.

ADJUST [40] relies on the joint use of spatial and temporal features to reject EEG artifacts. It maximizes the likelihood (ML) of observed data to classify eye blinks, horizontal and vertical eye movements and generic discontinuities based on five spatial and temporal statistical properties of the artifacts. Once a component is classified as an artefact, it is rejected. ADJUST reported its superior performance in terms of artifacts classification accuracy and neat EEG signal reconstruction when compared to manual artifacts removal techniques that rely on domain experts.

MARA [45] is a supervised linear classifier with six IC features collected from 35 subjects and 3 EEG paradigms to classify artifacts components and EEG components. Adapted strategy is also proposed to generalize for different electrode setups. The performance of this method in handling multiple artifacts has been evaluated against human expert ratings. It is reported to

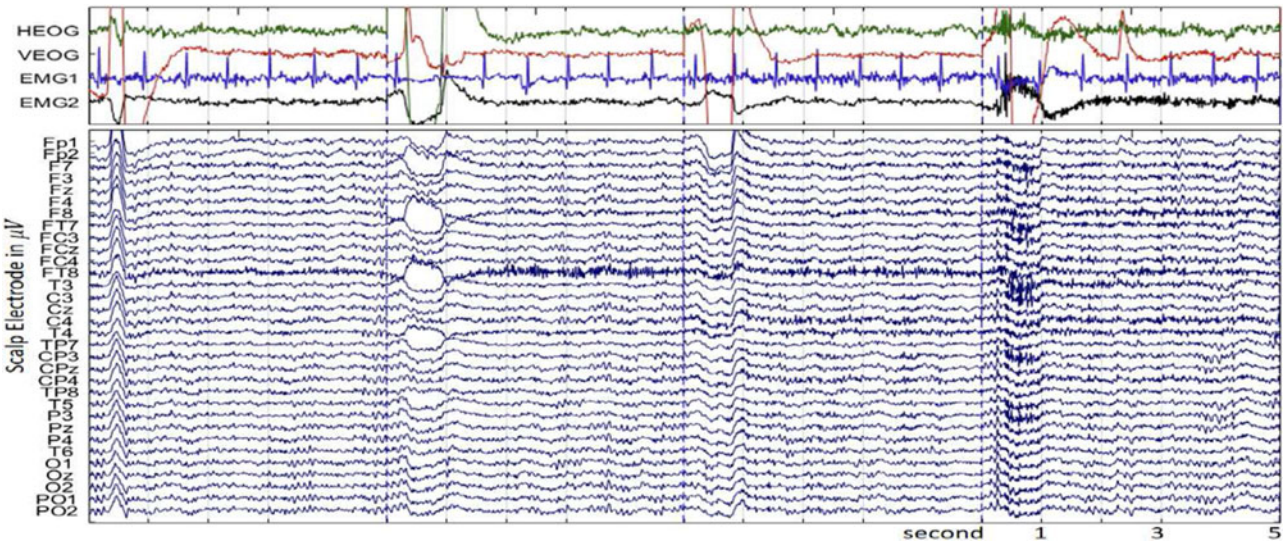

Fig. 1. Eye blink (EB), horizontal eye movement (HEM), vertical eye movement (VEM) and uttering 'Weee' (UW).

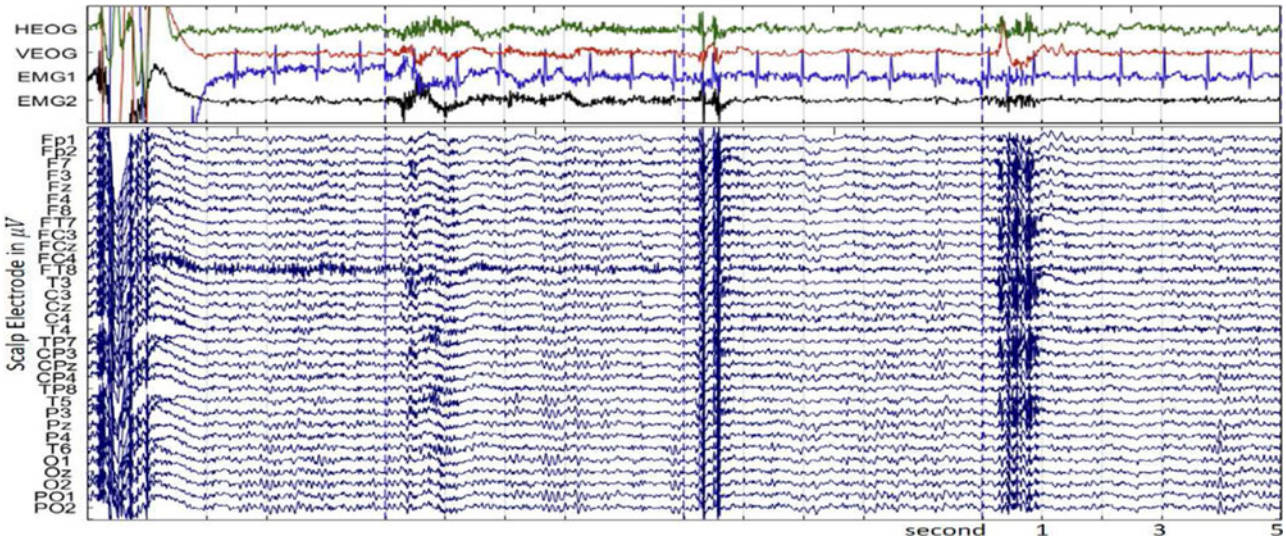

Fig. 2. Head shaking movement (HSM), swallowing, teeth tapping (TT) and grinding teeth (GT).

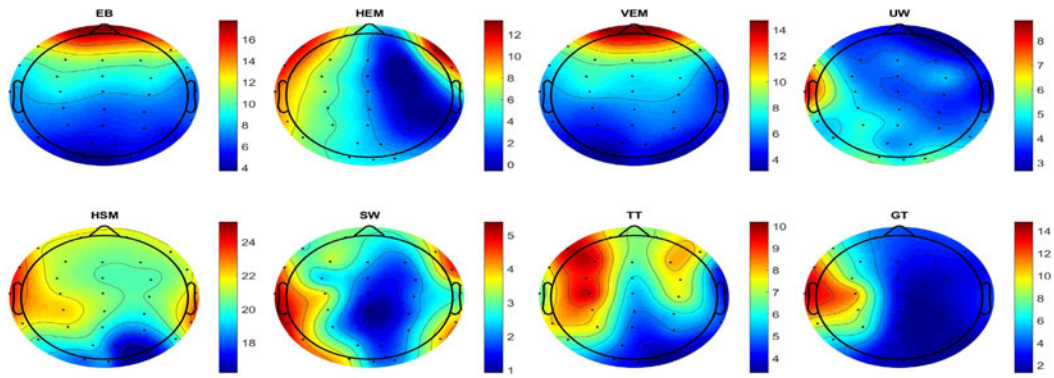

Fig. 3. EEG topographic map of Clutter-to-Signal Ratio (CSR) in decibel (dB).

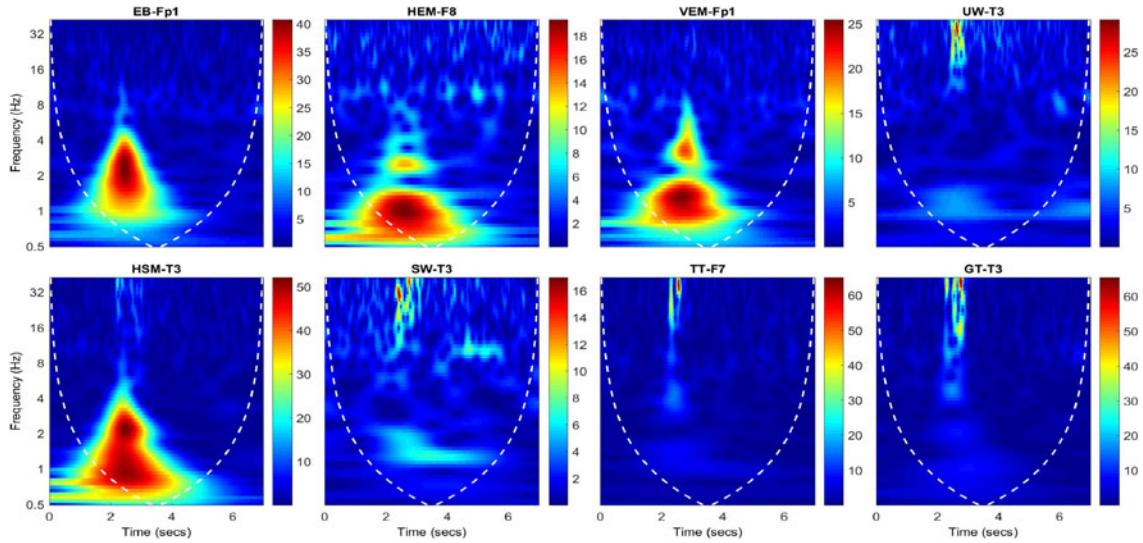

Fig. 4. Continuous wavelet transform (CWT) scalogram of the signal before applying ART. The dashed line is called cone of influence which shows where edge effects of the CWT become significant.

have maintained the integrity of the BCI performance while removing artifactual components.

wICA [23] hybridizes discrete wavelet transform with ICA for artifacts removal. It has a contrary goal to wavelet denoising where useful EEG has low amplitude while artifacts have higher amplitude. A wavelet thresholding to IC with a threshold similar to the one reported in [48] to estimate the contamination in the signal, is subtracted from that IC. It is reported to preserve both spectral (amplitude) and coherence (phase) characteristics of the underlying neural activity.

III. Methodology

After characterizing EEG artifacts and their spatial-temporal-spectral influence in EEG recording, our two proposed ARTs for removing multiple EEG artifacts are described. The studied artifacts are as follows:

A. EEG Tasks

1) Eye Blink Artifact (EB): A common artifact that has been studied significantly in EEG artifact removal studies. It is produced by closing of the eyelid then opening it.

2) Horizontal Eye Movement Artifact (HEM): A common, mostly voluntarily, behavioral pattern during information scanning on an interface or during naturally occurring interactions.

3) Vertical Eye Movement Artifact (VEM): It is another common and mostly voluntarily behavioral pattern during information scanning and naturally occurring interactions. It is used to signify a state of surprise or wonder.

4) Head Shaking Movement Artifact (HS): The shaking of one's head, vertically, horizontally or in both directions, is a common body movement in daily activities. In some cultures, the vertical head shaking signifies an agreement, while in other cultures, pushing the head up signifies a 'no'.

5) Uttering the Word 'Weee' Artifact (UW): It is common in daily activities that mouth muscles are used, either for speech production purposes or for non-verbal communications as in the case of producing a smile. This artifact is induced by the subject uttering the word 'Weee', with the sequence of e's causing the mouth and lips to shape as a smile.

6) Swallowing Artifact (SW): It is both a voluntarily and involuntarily behavioral pattern.

7) Teeth Tapping Artifact (TT): Teeth tapping is both a voluntarily and involuntarily behavioral pattern. It can occur when a subject close the month.

8) Teeth Grinding Artifact (GT): It is an involuntarily movement produced by a number of people during sleeping. It is sometimes also produced voluntarily during normal activities and eating.

These eight different artifacts were selected carefully to cover the main artifacts that could be encountered in a real-world situation and under normal working conditions.

B. Characteristics of EEG Artifacts and its Influence

Figs. 1 and 2 show the enormous influence of multiple EEG artifacts on the recording. In order to quantify the influence, we used clutter-to-signal ratio (CSR) defined in Section IV and Equation 6. CSR is a measure in decibel (dB) that indicates the level of contamination in EEG compared to the baseline EEG which quantifies the amount of artifacts' influence. In Fig. 3, we show an example of the EEG topographic map of CSR for each artefact. Every artefact is observed to have a very distinct and diverse spatial influence in addition to different CSR.

The spectral characteristics of EEG artifacts are visualized using continuous wavelet transform (CWT) scalogram in Fig. 4 where electrodes with maximum CSR are chosen. CWT shows the time-frequency influence of EEG artifacts and captures their transient impacts. Ocular movements and eye blink are observed to have low frequency while mouth movements influence higher frequency. Head shaking movements have a wider spectral influence. The summary of spectral and spatial

TABLE I
CHARACTERISTICS OF EEG ARTIFACTS. F - FRONTAL, T-TEMPORAL

	Entropy	Skewness	Kurtosis	Frequency	Region
EB	2.630	3.673	19.820	0–6 Hz	F
HEM	3.781	0.648	5.003	0–4 Hz	F
VEM	2.633	0.202	7.535	0–8 Hz	F
UW	3.890	−1.416	8.162	>16 Hz	T
HSM	2.510	−2.843	13.525	0–8 & >16 Hz	T
SW	3.495	−0.278	5.025	>12 Hz	T
TT	2.916	−3.980	40.421	>16 Hz	F, T
GT	3.157	−3.149	23.206	>12 Hz	T

influence along with several statistical measures for outlier-prone data, entropy, skewness and kurtosis, are summarized in Table I.

C. Proposed Artifacts Removal Techniques

In this work, we proposed two automated ARTs that work in conjunction with ICA. They are designed to manipulate the influence of EEG artifacts. They involve variance estimation of baseline EEG, artifacts segmentation, artifacts' influence detection, influence analysis, artifacts components removal and signal reconstruction from useful components.

Variance estimation of baseline EEG is achieved by computing the sliding singular value decomposition with window size of 500 ms and 50% overlapping. Assuming that at least 10% of the data is artifacts free, the variance, V_c, of each channel c can be computed using 10% of the data with the smallest first singular value. In other experimental design, a higher percentage can be chosen if artifact prevention procedure is followed while a lower percentage can always be used if percentage is hardly known. The baseline EEG can be enlarged by appending EEG segments with standard deviation that is not statistically twice larger than $\sqrt{V_c}$. This is achieved using one-tailed F-test (OTFT-n) of variance with the null hypothesis of variables x, ny having the same variance against the alternative that variance of x is n^2 times greater than that of y. The variance of the baseline V_b is computed using the enlarged baseline segment. When the baseline segments are removed from the data, it is left with EEG segment that are suspicious for artifacts contamination. Each suspicious segment is extended with 250 ms on each end.

For each suspicious segment EEG_s, an influence analysis is performed to determine if there is an artefact in the signal. The most influential component will be removed and $\widehat{EEG_s}$ will be reconstructed using the remaining components, when the influence of the artifacts is detected. This step repeats until the variance of $\widehat{EEG_s}$ accepts the null hypothesis of OTFT-2 compared to the V_b.

We defined two ways to model the strength of influence, **H1** and **H2**, as follow:

1) H1: It is designed based on Pearson correlation that measures the similarity of component between ith IC S_i and cth signal X_c. This method has been tested on synthetic data set in [50]. We have H1 as follows:

$$H1(S_i) = \sum_{c}^{C} corr(S_i, X_c))^2 \tag{1}$$

C is the set of channels in favor of alternative hypothesis of OTFT-1 compared to V_b. The most influential component S_f is selected based on:

$$f = \arg\max_{f}(H1(S_f)) \tag{2}$$

The additional condition of removing S_f is that $H1(S_f) > 1$ as set in [50].

2) H2: The second model analyses the function $f_{c,i}$ from ICA that $f : S_i \mapsto X_c$. The value of X_c is bounded by minkowski sum of $I_{c,i}\ \forall i$ where $I_{c,i}$ is the interval of $\hat{X}_c$ reconstructed from S_i. $I_{c,i} = [\min(f_{c,i}(S_i)), \max(f_{c,i}(S_i))]$.

H2 is defined as follows:

$$H2(S_i, c) = I_{c,i} \tag{3}$$

For each X_c, there is a k where

$$k_c = \arg\max_{k}(H2(S_k, c)) \tag{4}$$

The most influential component S_f is selected to be $f = mode(k_c)$ where the mode of a set equals the element that occurs most in the set. Similar to H1, $c \in C$ is the set of channels in favor of alternative hypothesis of OTFT-1 compared to V_b.

IV. CRITERIA FOR VALIDATION

In order to ensure the reliability of EEG system, validating the performance of EEG ARTs is indispensable. Several performance metrics have been proposed to validate ARTs [12]. Four criteria, that validate both temporal and spectral content of the signal, are used in this study to assess ARTs for synthesized and acquired EEG.

Synthesized EEG artifacts has the advantage that the performance can be assessed using standardized metrics [12]. Signal-to-noise ratio (SNR) is used to validate the ARTs on synthesized artifacts.

$$SNR = 10 \times \log_{10}\left(\frac{P_{signal}}{P_{noise}}\right) \tag{5}$$

Furthermore, artifact residue (AR) and information loss (IL) of the synthesized data in frequency domain are proposed as new metrics. They are defined as the area between the power spectral density (PSD) curves of the processed EEG and ground truth EEG. Artifact residue captures the additional signal added to the signal. It is defined as the area above ground truth, while information loss is the area below the ground truth capturing the removal of EEG content.

For acquired EEG, the performance of each ART will be evaluated using clutter-to-signal ratio (CSR) and time-frequency analysis and visualization. Clutter-to-signal ratio (CSR) is defined as follows:

$$CSR_i = 10 \times \log_{10}(R) = 10 \times \log_{10}\left(\frac{P_i}{P_f}\right) \tag{6}$$

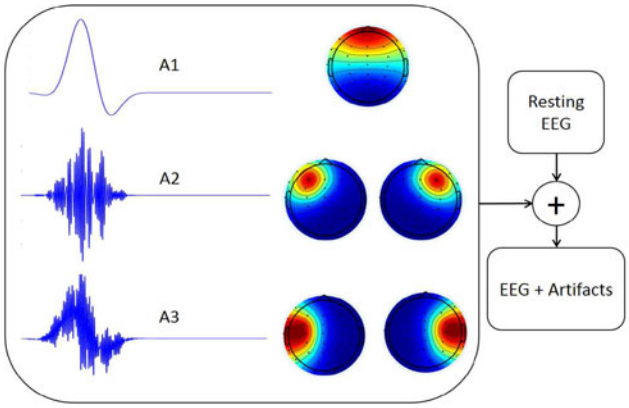

Fig. 5. Synthesis of EEG artifacts.

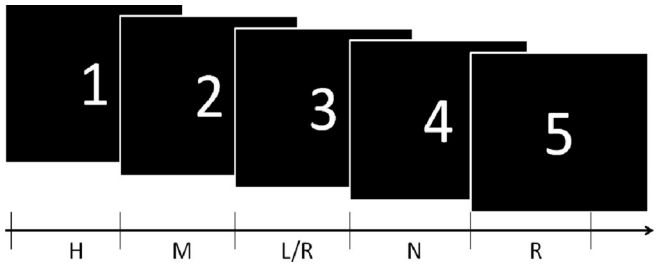

Fig. 6. The timeline for each trial. The subjects are requested to induce the required artifact while controlling for all other artifacts starting from the first second. The amount of the artifact influence to each second is categorized into five categories: high(H), medium(M), low(L), rare(R), neutral(N). The neutral category represents the absence of knowledge on the amount of artifact in the fifth second because subjects are expected to be in a state whereby they are anticipating the induction of the artifact in the following first second.

where P_i is the power of signal i, P_f is the power of the signal that is artefact-free. CSR is a modification of signal to noise ratio (SNR). CSR is adopted here because the ground truth of EEG is unavailable and noise (artifact) has larger amplitude compared to the signal of interest. An ART that handles multiple artifacts well will have a CSR score closer to 0, while removing too much information will make CSR much smaller than 0.

The second criteria of acquired EEG is based on time-frequency analysis of the processed EEG signal. CWT scalogram is adopted in this study. Compared to CSR and distortion in frequency bands in [24], CWT has the advantage of having higher spectral and temporal resolution; thus, a small artifact residuals can still be easily visualized.

V. Synthesized EEG Artifacts

In this study, we synthesized three type of EEG artifacts (A1, A2, A3) in Fig. 5 using Morlet wavelet [51]. Artifact A_i is synthesized by tuning the wavelet coefficients at different scales and location to obtain signal with desired signal-to-noise ratio (SNR), duration (1–2s), amplitude and frequency. A1 and A2 are low (0-8 Hz) and high (16-42 Hz) frequency artifacts while A3 is a mixture of them. The spatial propagation of EEG artifacts are assumed to have strength/amplitude decrease exponentially as it traverses. The synthesized artifacts are then added to the acquired resting state EEG.

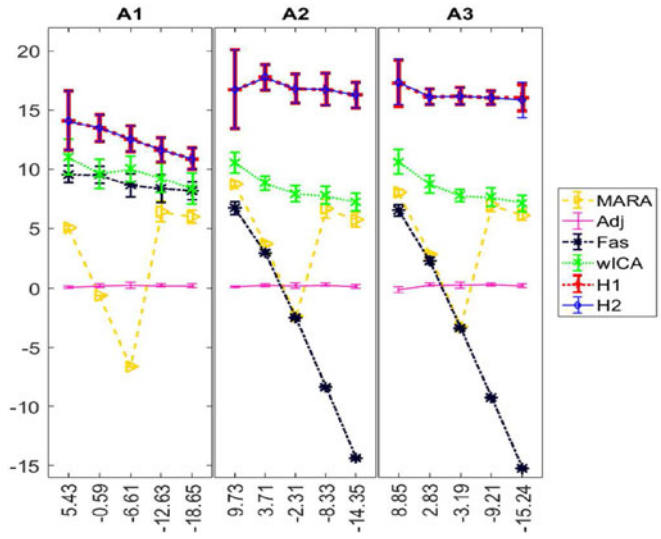

Fig. 7. Signal-to-noise ratio of the processed signal before (x-axis) and after (y-axis) applying ARTs.

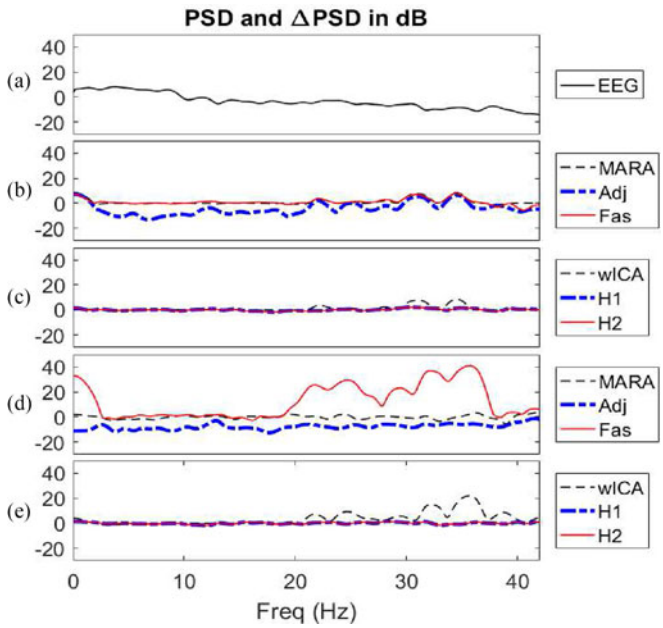

Fig. 8. (a) Power spectral density (PSD) of the ground truth EEG. (b) & (c) The PSD difference between processed A3 with r = 1 and ground truth EEG. (d) & (e) The PSD difference between processed A3 with r = 16 and ground truth EEG.

For each type of artifact A_i, 30 trials are generated for different SNR. An decreasing SNR of the synthesized artifacts are achieved by setting the standard deviation of EEG artifacts to be r times larger than the average standard deviation of the resting EEG. $r = 1, 2, 4, 8, 16$ are investigated. The average SNR for each A_i can be found in the x-axis in Fig. 7.

VI. Experimental Protocol

Six subjects are used in this experiment. Two sessions were performed. In each session, the eight different experiments representing the eight individual artifacts were conducted. Each

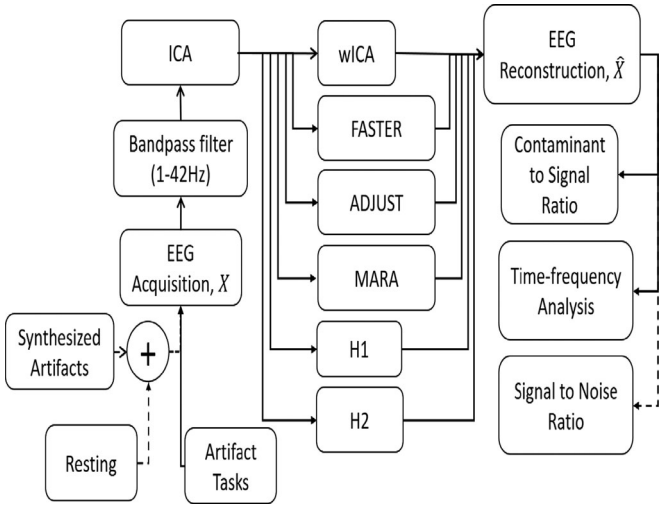

Fig. 9. Experimental Design for assessment and validation EEG artifact processing techniques.

experiment for each artifact (epoch) lasted for five seconds, and is repeated 30 times. This roughly equated to 1.5 hours between testing each artifact in the first session and retesting it in the second session. All experiments were conducted in a single 3-hour block without any breaks in between. In each epoch, the subject was faced with a black screen and a counter in the middle. The counter starts from 1, signalling to the subject that a single occurrence of the required artifact needs to be induced, and continues to 5 with an increment of 1. The timeline for each epoch is summarized in Fig. 6. Once the counter reaches 5, it starts again from 1. The inter-counting time is fixed to 1 second, thus each epoch lasts for 5 seconds and all artifact were induced at the start of each epoch. The subject controlled for all other artifacts, was monitored by an analyst to provide a secondary validation for the control, and was video tapped for post-check.

To validate the five second design discussed above, Fig. 4 shows the continuous wavelet transform scalogram of signal from -2 to 5 second at the channel where CSR is maximum. Comparing the observation in each second to the fourth second, the largest differences are observed in the first two seconds, which are very different for different type of artifact. However, this trend changes in the third and fifth seconds. The data were collected using Neuroscan NuAmps, a 32 channel EEG Amplifier, with a sampling rate of 250 Hz in a continuous recording mode. EOG and EMG were recorded for post-check. The EMG was recorded from two locations: from the back of the neck underneath the Inion, and the second on the left Masseter muscle. Events were tagged to mark the beginning and end of each five second epochs, which are then extracted for post processing.

VII. Experiments and Results

Fig. 9 shows the flow for data processing starting with the acquisition of EEG signals and synthesis of EEG artifact in their raw forms without segmentation based on types to test the capability of ARTs in the scenario of multiple artifacts. They are then bandpass filtered between 1 Hz and 42 Hz. Extended informax ICA is then performed on the filtered data to estimate independent sources. wICA, FASTER, ADJUST, MARA, H1 and H2 are used for artifact removal. Eventually, the processed signals are reconstructed and evaluated using four criteria discussed in IV.

TABLE II
Artifact Residue and Information Loss of A3 Before and After Applying ARTs

r	1		16	
Algo	AR	IL	AR	IL
EEG + A3	54.66	−1.77	529.99	−2.64
MARA	54.19	−8.07	24.39	−31.52
Adj	39.05	−206.41	0.00	−317.41
Fas	60.04	−10.47	534.93	−9.15
wICA	44.62	−3.82	157.27	−7.34
H1	15.07	−16.88	13.09	−15.59
H2	15.07	−16.88	13.09	−15.59

Fig. 7 summarized the SNR performance of ARTs on synthesized EEG artifacts. H1 and H2 are observed to have superior performance comparing to all other methods. wICA performed better and was more reliable for different SNR compared to MARA, ADJUST and FASTER. MARA is only reliable when SNR is high and had false negative when SNR is low. FASTER can only handle A1 artifact, while ADJUST failed to handle all synthesized artifacts. Fig. 8 shows the power spectral density (PSD) of the ground truth EEG and the PSD difference between the processed EEG and ground truth EEG for A3 artifact with r = 1 and 16 at channel C3. The artifact residue (AR) and information loss (IL) defined in Section IV are summarized in Table II. H1 and H2 achieved a better trade off between artifact removal and information loss for synthesized EEG, for having the smallest $|AR| + |IL|$. The similarity in performance of H1 and H2 indicated that both heuristics identified nearly the same influential ICs for synthesized artifacts.

In Fig. 10, the box plot of CSR in decibel (dB) of all acquired EEG channels before and after artifact processing for all subjects are shown. Five auxiliary lines (a, b, c, d, e) are drawn to indicate the power ratio R in equation 6. ADJUST was found to have a large CSR in some cases, while having very small CSR for others. It fails by maintaining a level of artifact while removing genuine EEG information. FASTER performed better than ADJUST, although there is still a large artifact residual in the processed signal. Both FASTER and ADJUST have failed significantly in this multiple EEG artifact circumstance. MARA was found to remove many artifacts as well as EEG information as demonstrated by the low CSR for some cases. wICA was having the best CSR compared to ADJUST, FASTER and MARA, especially for ocular and eye blink artifacts.

H1 and H2 were observed to have CSR that falls within line a to line c for most of the artifacts and the 25th to 75th percentiles of the CSR are very close to 0; which is a good indication of artifact removal while retaining EEG information. A few exceptions of low CSR were due to the limitation of ICA where contaminated signals are separated into multiple ICs. In Fig. 11,

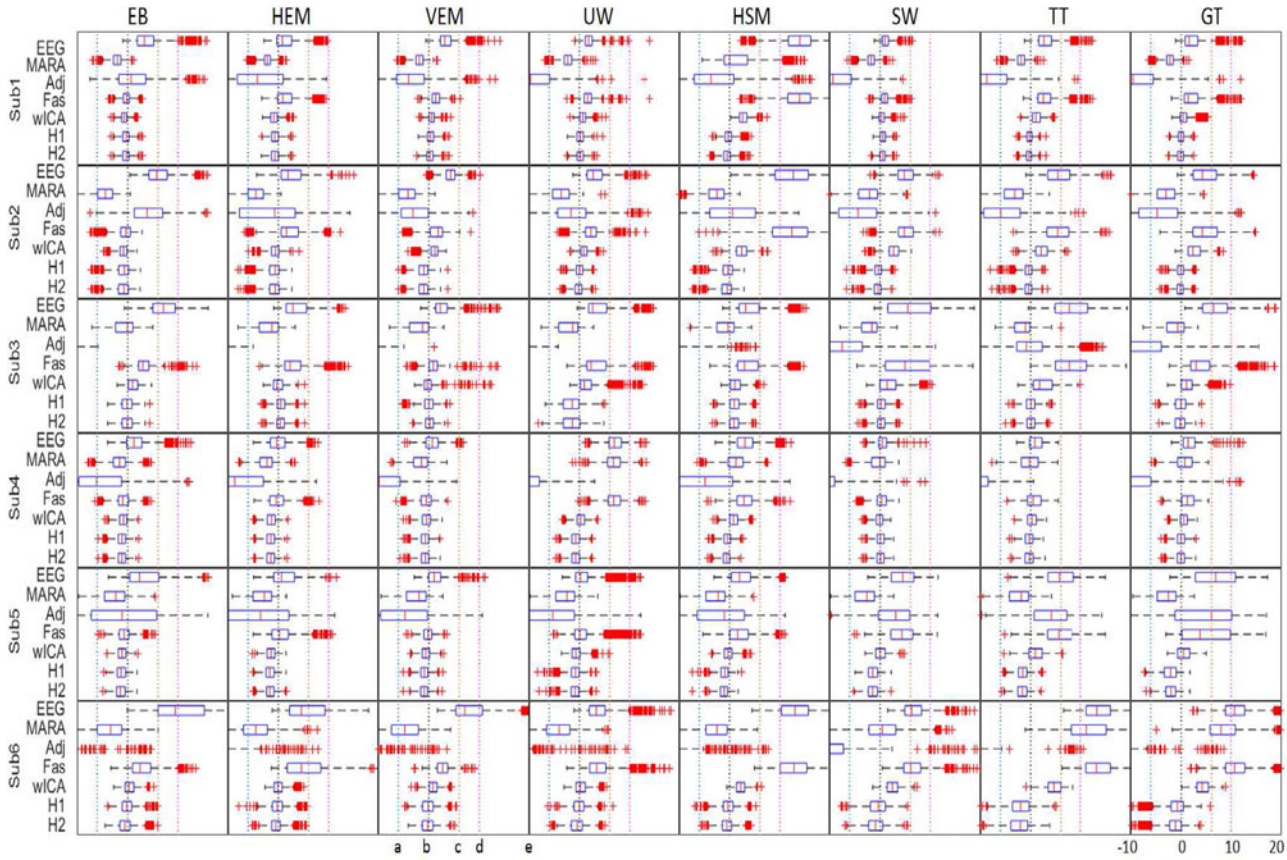

Fig. 10. The box plot of Clutter-to-Signal Ratio (CSR) in decibel (dB) (Equation 6) for all EEG channels of EEG artifacts before and after applying ARTs. The auxiliary line a, b, c, d and e indicate CSR where R = 0.25, 1, 4, 10 and 100.

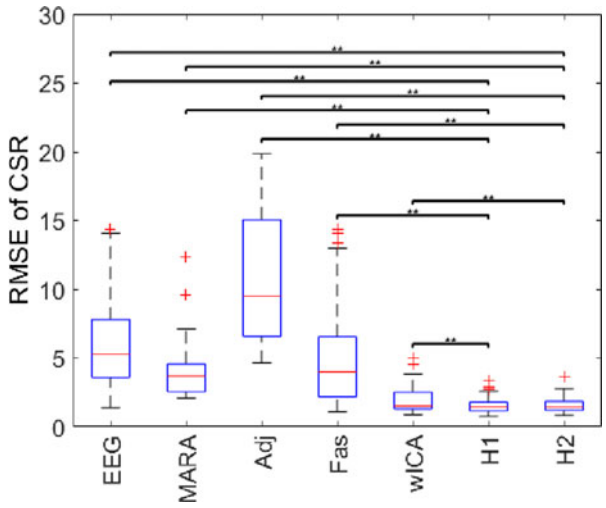

Fig. 11. Root-mean-square error (RMSE) of CSR for each ART. All ARTs are compared to H1 and H2 using one-tailed paired-sample T-test (** for $p < 0.01$). Wilcoxon signed rank test gave the results of $p < 0.01$, except for wICA where $p < 0.05$.

the root-mean-square error (RMSE) of CSR are shown. H1 and H2 are found to have statistical significant and better RMSE using one-tailed paired-sample T-test and Wilcoxon signed rank test compared to all other ARTs.

The time-frequency analysis of the processed data for all six ART are shown in Figs. 1–6 in the supplemental materials. ADJUST and FASTER are observed to have eliminated little artifact, yet they are far from exhibiting a satisfactory performance across all artifact. MARA is observed to remove 6 types of artifacts well except for head shaking and teeth tapping. wICA handled the ocular artifact and eye blink while having artifact residues for all others. H1 reduces the influence of all artifact although there is a residue in swallowing and teeth tapping. In time frequency analysis, H2 was performing best for all 8 types of artifact with a small artifact residue in head shaking movement and uttering 'wee'.

Combining the result from synthesized and acquired EEG, H2 is found to be the most reliable and robust to all 8 types of EEG artifacts studied in this work. From the results, some insights can be drawn: (1) H1 and H2 have a few assumptions that make them generalize better to different types of artifacts (2) there is a trade off between information loss and artifact removal as every component that is used to model artifact sources will reduce the rank of EEG data by 1. The situation is worsen when contaminated signals are separated into multiple ICs (3) A more advanced BSS is required as the ability of ICA to specialize the components to EEG and artifact information is not perfect. This ability is limited by the fact that the number of estimated sources equals to the number of EEG channel.

VIII. Conclusion

There are three complimentary goals achieved in these studies: (1) characterize the spatiotemporal-frequency influence of EEG artifacts collected from 8 carefully designed experimental scenarios, (2) evaluate existing automated artifact removal techniques in the scenario of multiple artifacts using both acquired and synthesized EEG, (3) design robust artifact removal techniques that have fewer restrictive prior assumption on artifact characteristics to be generalizable to handle several type of artifacts in the scenario of multiple artifacts.

Two of our proposed ARTs, that model and manipulate artifact influence through influential independent components, achieved a superior signal-to-noise (SNR) in synthesized data and better clutter-to-signal ratio (CSR) score for all 6 subjects in acquired EEG and showed better artifact processing in time-frequency analysis and visualization for 8 types of artifacts compared to four other methods. By reconstructing a higher quality signal from artifact contamination, this work facilitates reliable clinical EEG analysis and robust BCI system.

Our future work will extend the influence analysis to the artifact removal techniques that combine BSS and wavelet/EMD, which have been reported to produce improved results, and to achieve a more precise automated EEG and artifact separation.

References

[1] J. R. Wolpaw, N. Birbaumer, D. J. McFarland, G. Pfurtscheller, and T. M. Vaughan, "Brain–computer interfaces for communication and control," *Clin. Neurophysiol.*, vol. 113, no. 6, pp. 767–791, 2002.

[2] M. Arvaneh, C. Guan, K. K. Ang, and Q. Chai, "Optimizing spatial filters by minimizing within-class dissimilarities in electroencephalogram-based brain-computer interface," *IEEE Trans. Neural Netw. Learn. Syst.*, vol. 24, no. 4, pp. 610–619, Apr. 2013.

[3] H. Zhang, H. Yang, and C. Guan, "Bayesian learning for spatial filtering in an EEG-based brain–computer interface," *IEEE Trans. Neural Netw. Learn. Syst.*, vol. 24, no. 7, pp. 1049–1060, Jul. 2013.

[4] H. Cecotti, M. P. Eckstein, and B. Giesbrecht, "Single-trial classification of event-related potentials in rapid serial visual presentation tasks using supervised spatial filtering," *IEEE Trans. Neural Netw. Learn. Syst.*, vol. 25, no. 11, pp. 2030–2042, Nov. 2014.

[5] R. Khosrowabadi, C. Quek, K. K. Ang, and A. Wahab, "ERNN: A biologically inspired feedforward neural network to discriminate emotion from EEG signal," *IEEE Trans. Neural Netw. Learn. Syst.*, vol. 25, no. 3, pp. 609–620, Mar. 2014.

[6] J. Hu, H. Tang, K. C. Tan, and H. Li, "How the brain formulates memory: A spatio-temporal model research frontier," *IEEE Comput. Intell. Mag.*, vol. 11, no. 2, pp. 56–68, May 2016.

[7] H. Abbass, J. Tang, R. Amin, M. Ellejmi, and S. Kirby, "The computational air traffic control brain: Computational red teaming and big data for real-time seamless brain-traffic integration," *J. Air Traffic Control*, vol. 56, no. 2, pp. 10–17, 2014.

[8] H. A. Abbass, J. Tang, R. Amin, M. Ellejmi, and S. Kirby, "Augmented cognition using real-time EEG-based adaptive strategies for air traffic control," *Proc. Human Factors Ergonom. Soc. Annu. Meeting*, vol. 58, no. 1, pp. 230–234, 2014.

[9] M. Kirkove, C. François, and J. Verly, "Comparative evaluation of existing and new methods for correcting ocular artifacts in electroencephalographic recordings," *Signal Process.*, vol. 98, pp. 102–120, 2014.

[10] R. J. Croft, J. S. Chandler, R. J. Barry, N. R. Cooper, and A. R. Clarke, "EOG correction: A comparison of four methods," *Psychophysiology*, vol. 42, no. 1, pp. 16–24, 2005.

[11] L. Sörnmo and P. Laguna, *Bioelectrical Signal Processing in Cardiac and Neurological Applications*, vol. 8. New York, NY, USA: Academic, 2005.

[12] J. A. Urigüen and B. Garcia-Zapirain, "EEG artifact removal-state-of-the-art and guidelines," *J. Neural Eng.*, vol. 12, no. 3, 2015, Art. no. 031001.

[13] G. L. Wallstrom, R. E. Kass, A. Miller, J. F. Cohn, and N. A. Fox, "Automatic correction of ocular artifacts in the EEG: A comparison of regression-based and component-based methods," *Int. J. Psychophysiol.*, vol. 53, no. 2, pp. 105–119, 2004.

[14] R. J. Croft and R. J. Barry, "Removal of ocular artifact from the EEG: A review," *Neurophysiologie Clinique/Clinical Neurophysiol.*, vol. 30, no. 1, pp. 5–19, 2000.

[15] K. T. Sweeney, T. E. Ward, and S. F. McLoone, "Artifact removal in physiological signals—Practices and possibilities," *IEEE Trans. Inf. Technol. Biomed.*, vol. 16, no. 3, pp. 488–500, May 2012.

[16] S. Romero, M. Mañanas, and M. J. Barbanoj, "Ocular reduction in EEG signals based on adaptive filtering, regression and blind source separation," *Ann. Biomed. Eng.*, vol. 37, no. 1, pp. 176–191, 2009.

[17] C. Marque, C. Bisch, R. Dantas, S. Elayoubi, V. Brosse, and C. Perot, "Adaptive filtering for ECG rejection from surface EMG recordings," *J. Electromyogr. Kinesiol.*, vol. 15, no. 3, pp. 310–315, 2005.

[18] R. Sameni, M. B. Shamsollahi, C. Jutten, and G. D. Clifford, "A nonlinear Bayesian filtering framework for ECG denoising," *IEEE Trans. Biomed. Eng.*, vol. 54, no. 12, pp. 2172–2185, Dec. 2007.

[19] F. Morbidi, A. Garulli, D. Prattichizzo, C. Rizzo, and S. Rossi, "Application of Kalman filter to remove TMS-induced artifacts from EEG recordings," *IEEE Trans. Control Syst. Technol.*, vol. 16, no. 6, pp. 1360–1366, Nov. 2008.

[20] M. Unser and A. Aldroubi, "A review of wavelets in biomedical applications," *Proc. IEEE*, vol. 84, no. 4, pp. 626–638, Apr. 1996.

[21] N. E. Huang *et al.*, "The empirical mode decomposition and the hilbert spectrum for nonlinear and non-stationary time series analysis," in *Proc. Roy. Soc. London A, Math., Phys. Eng. Sci.*, vol. 454, no. 1971, pp. 903–995, 1998.

[22] M. T. Akhtar, W. Mitsuhashi, and C. J. James, "Employing spatially constrained ICA and wavelet denoising, for automatic removal of artifacts from multichannel EEG data," *Signal Process.*, vol. 92, no. 2, pp. 401–416, 2012.

[23] N. P. Castellanos and V. A. Makarov, "Recovering EEG brain signals: Artifact suppression with wavelet enhanced independent component analysis," *J. Neurosci. Methods*, vol. 158, no. 2, pp. 300–312, 2006.

[24] V. Bono, S. Das, W. Jamal, and K. Maharatna, "Hybrid wavelet and EMD/ICA approach for artifact suppression in pervasive EEG," *J. Neurosci. Methods*, vol. 267, pp. 89–107, 2016.

[25] D. Safieddine *et al.*, "Removal of muscle artifact from EEG data: Comparison between stochastic (ICA and CCA) and deterministic (EMD and wavelet-based) approaches," *EURASIP J. Adv. Signal Process.*, vol. 2012, no. 1, pp. 1–15, 2012.

[26] D. Looney, L. Li, T. M. Rutkowski, D. P. Mandic, and A. Cichocki, "Ocular artifacts removal from EEG using EMD," in *Proc. Adv. Cogn. Neurodyn.*, 2008, pp. 831–835.

[27] M. K. Molla, T. Tanaka, T. M. Rutkowski, and A. Cichocki, "Separation of EOG artifacts from EEG signals using bivariate EMD," in *Proc. IEEE Int. Conf. Acoust., Speech Signal Process*, 2010, pp. 562–565.

[28] S. K. Goh, H. A. Abbass, K. C. Tan, A. Al-Mamun, C. Guan, and C. C. Wang, "Multiway analysis of EEG artifacts based on block term decomposition," in *Proc. Int. Joint Conf. Neural Netw.*, 2016, pp. 913–920.

[29] P. Berg and M. Scherg, "Dipole modelling of eye activity and its application to the removal of eye artefacts from the EEG and MEG," *Clin. Phys. Physiol. Meas.*, vol. 12, 1991, Art. no. 49.

[30] W. De Clercq, A. Vergult, B. Vanrumste, W. Van Paesschen, and S. Van Huffel , "Canonical correlation analysis applied to remove muscle artifacts from the electroencephalogram," *IEEE Trans. Biomed. Eng.*, vol. 53, no. 12, pp. 2583–2587, Nov. 2006.

[31] P. Comon, "Independent component analysis, a new concept?" *Signal Process.*, vol. 36, no. 3, pp. 287–314, 1994.

[32] D. Langlois, S. Chartier, and D. Gosselin, "An introduction to independent component analysis: InfoMax and FastICA algorithms," *Tut. Quant. Methods Psychol.*, vol. 6, no. 1, pp. 31–38, 2010.

[33] Y. Li, Z. Ma, W. Lu, and Y. Li, "Automatic removal of the eye blink artifact from EEG using an ICA-based template matching approach," *Physiol. Meas.*, vol. 27, no. 4, pp. 425–436, 2006.

[34] A. Belouchrani, K. Abed-Meraim, J.-F. Cardoso, and E. Moulines, "A blind source separation technique using second-order statistics," *IEEE Trans. Signal Process.*, vol. 45, no. 2, pp. 434–444, Feb. 1997.

[35] A. J. Bell and T. J. Sejnowski, "An information-maximization approach to blind separation and blind deconvolution," *Neural Comput.*, vol. 7, no. 6, pp. 1129–1159, 1995.

[36] A. Hyvärinen and E. Oja, "Independent component analysis: algorithms and applications," *Neural Netw.*, vol. 13, no. 4, pp. 411–430, 2000.
[37] J. Himberg and A. Hyvarinen, "Icasso: software for investigating the reliability of ICA estimates by clustering and visualization," in *Proc. IEEE 13th Workshop Neural Netw. Signal Process.*, 2003, pp. 259–268.
[38] T.-W. Lee, M. Girolami, and T. J. Sejnowski, "Independent component analysis using an extended infomax algorithm for mixed subgaussian and supergaussian sources," *Neural Comput.*, vol. 11, no. 2, pp. 417–441, 1999.
[39] J. N. Demos, *Getting Started With Neurofeedback*. New York, NY, USA: Norton, 2005.
[40] A. Mognon, J. Jovicich, L. Bruzzone, and M. Buiatti, "ADJUST: An automatic EEG artifact detector based on the joint use of spatial and temporal features," *Psychophysiology*, vol. 48, no. 2, pp. 229–240, 2011.
[41] R. Vigário, V. Jousmäki, M. Hämäläninen, R. Hari, and E. Oja, "Independent component analysis for identification of artifacts in magnetoencephalographic recordings," in *Proc. Conf. Adv. Neural Inf. Process. Syst.*, 1998, pp. 229–235.
[42] K. T. Sweeney, S. F. McLoone, and T. E. Ward, "The use of ensemble empirical mode decomposition with canonical correlation analysis as a novel artifact removal technique," *IEEE Trans. Biomed. Eng.*, vol. 60, no. 1, pp. 97–105, Jan. 2013.
[43] B. Mijovic, M. De Vos, I. Gligorijevic, J. Taelman, and S. Van Huffel, "Source separation from single-channel recordings by combining empirical-mode decomposition and independent component analysis," *IEEE Trans. Biomed. Eng.*, vol. 57, no. 9, pp. 2188–2196, Sep. 2010.
[44] H. Nolan, R. Whelan, and R. Reilly, "FASTER: Fully automated statistical thresholding for EEG artifact rejection," *J. Neurosci. Methods*, vol. 192, no. 1, pp. 152–162, 2010.
[45] I. Winkler, S. Brandl, F. Horn, E. Waldburger, C. Allefeld, and M. Tangermann, "Robust artifactual independent component classification for BCI practitioners," *J. Neural Eng.*, vol. 11, no. 3, 2014, Art. no. 035013.
[46] V. Lawhern, W. D. Hairston, and K. Robbins, "Detect: A matlab toolbox for event detection and identification in time series, with applications to artifact detection in EEG signals," *PloS One*, vol. 8, no. 4, 2013, Art. no. e62944.
[47] S. Makeig, M. Westerfield, T.-P. Jung, S. Enghoff, J. Townsend, E. Courchesne, and T. Sejnowski, "Dynamic brain sources of visual evoked responses," *Science*, vol. 295, no. 5555, pp. 690–694, 2002.
[48] T.-P. Jung *et al.*, "Removing electroencephalographic artifacts by blind source separation," *Psychophysiology*, vol. 37, no. 2, pp. 163–178, 2000.
[49] D. L. Donoho, I. M. Johnstone, G. Kerkyacharian, and D. Picard, "Wavelet shrinkage: Asymptopia?" *J. Roy. Statist. Soc. B, Methodol.*, vol. 57, pp. 301–369, 1995.
[50] H. A. Abbass, "Calibrating independent component analysis with Laplacian reference for real-time EEG artifact removal," in *Proc. Int. Conf. Neural Inf. Process.*, 2014, pp. 68–75.
[51] A. Teolis, *Computational Signal Processing With Wavelets*. New York, NY, USA: Springer, 2012.

Sim Kuan Goh received the B.Eng. degree in electrical engineering from the National University of Singapore, Singapore, in 2013. He is currently working toward the Ph.D. degree in control, intelligent systems and Robotics in the Department of Electrical and Computer Engineering, National University of Singapore. His research interests include computational intelligence, machine learning, and brain computer interface.

Hussein A. Abbass is currently a Full Professor at the University of New South Wales, Canberra Campus, Canberra, ACT, Australia. He has published more than 200 refereed papers. His current research focuses on machine trust for trusted autonomy, where he designs next generation trusted autonomous systems. He is a Fellow of the U.K. Operational Research Society and a Fellow of the Australian Computer Society. He is the Vice-President of the Technical Activities (2016–2017) of IEEE-CIS and the National President (2016–present) of the Australian Society for Operations Research. He is an Associate Editor of six international journals.

Kay Chen Tan is currently a Full Professor in the Department of Computer Science, City University of Hong Kong, Hong Kong. He has published more than 200 refereed articles and five books. From 2010 to 2013, he was the Editor-in-Chief of the IEEE COMPUTATIONAL INTELLIGENCE MAGAZINE and is currently the Editor-in-Chief of the IEEE TRANSACTIONS ON EVOLUTIONARY COMPUTATION. He currently serves on the Editorial Board of more than 20 journals. He is an elected member of the IEEE CIS AdCom (2017–2019) and is an IEEE CIS Distinguished Lecturer (2015–2017).

Abdullah Al-Mamun received the Graduation degree from the Indian Institute of Technology Kharagpur, Kharagpur, India, in 1985, and the Ph.D. degree from the National University of Singapore, Singapore, in 1997. He is currently an Associate Professor in the Department of Electrical and Computer Engineering, National University of Singapore. He has published about 50 journal papers and about 60 papers in conference proceedings, and coauthored one book. His research interests include precision servomechanism, intelligent control, and robotics.

Chuanchu Wang received the Bachelor's and Master's degrees from the Electrical Engineering Department, University of Science and Technology of China, Hefei, China, in 1988 and 1991, respectively. He is currently a Principle Engineer in the Institute for Infocomm Research (I2R), Agency for Science (A*STAR), Technology and Research, Singapore. His current work at I2R is on the research and development of brain–computer interface based applications on assistive device, rehabilitation trials, and gaming.

Cuntai Guan is currently a Professor at the Nanyang Technological University, Singapore, the Principal Scientist in the Institute for Infocomm Research, Singapore, and the Co-Director of Rehabilitation Research Institute of Singapore, Singapore. He is on the Editorial Board of several journals. He has published more than 280 refereed journal and conference papers and holds 20 patents and applications. His research interests include brain–computer interfaces, neural engineering, machine learning, data analytics, and neuro-technology.